Supplementary Material

[18F]Fludarabine-PET as a promising tool for differentiating CNS lymphoma and glioblastoma: Comparative analysis with [18F]FDG in human xenograft models

Narinée Hovhannisyan[1], Fabien Fillesoye[1], Stéphane Guillouet[1], Méziane Ibazizene[1], Jérôme Toutain[2], Fabienne Gourand[1], Samuel Valable[2], Benoit Plancoulaine[3], Louisa Barré[1,*]

1. Normandie Univ, UNICAEN, CEA, CNRS, CHU Caen, ISTCT/LDM-TEP group, GIP Cyceron, Caen, France

2. Normandie Univ, UNICAEN, CEA, CNRS, CHU Caen, ISTCT/CERVOxy group, GIP Cyceron, Caen, France

3. Normandie Univ, UNICAEN, INSERM, ANTICIPE, Caen, France

* **Corresponding author**: Louisa Barré, ISTCT, LDM-TEP group, GIP Cyceron, Bd Henri Becquerel, BP 5229, 14074 Caen Cedex 5, France. Phone (33)231470224; fax (33)231470275; e-mail address barre@cyceron.fr

Supplementary Material

Data quantification methods

1. Global analysis using VOI (including manually defined ROIs) encompassing the entire tumor. This method was applied on 3D PET images to measure the levels of radiotracer uptake for inter-group comparisons between the radiotracers and the tumor models, as well as for TAC extraction. Note: the tumor was initially delineated on T2w scan (coronal plane) and transposed on PET by inversing the calculated R_c transform (R_c^{-1}) and the cerebellar tissue was initially defined on CT image and transposed on PET by inversing the R_2 transform (R_2^{-1}) (**Figure S1**); these VOI manipulations allowed performing the PET quantification on original PET images.

**2.** Specific analysis using tile-based method [41] to investigate the relationship between the PET activity calculated on 2D images and the quantitative values (tumor-cell density characterized with CD79) extracted from corresponding histological slides. For this, algorithms were developed to automatically segment the cancerous tissues on histological images and to make the correlation calculations as observer-independent as possible (**Figure S3**).

3. Global analysis setting ROI on 2D PET images to define the active tumoral area (ATA) by applying isocontour 41 % on the initial contours defined on T2w scans. The ATA was further correlated with MRI measurements of tumor area, as well as with CD79-stained surface determined on the corresponding histological section within the segmentation step of the method 2 (**Figure S3B**).

4. Local analysis fixed-size square shape ROIs. The mean activity calculated in the region was graded in function of tumor-cell density (**Figure S3E**): ROIs were defined on the co-registered density-image of the CD79 staining and projected on corresponding 2D PET, T1w-Gd and histological (CD68 & RECA) images. The tumor-cell density was sampled into three levels: tumor core (high density), peripheral tumor (intermediate) and normal tissue (low).

Note: The Gd related data (signal area and intensity) were defined on a difference image calculated between the latest frame (after administration) and the baseline frame (before administration) of the same T1w dynamic scan. This subtraction facilitates the detection of enhanced zones and permits to exclude the non-uniformity of signal in the image, appearing as bright areas close to the coil.
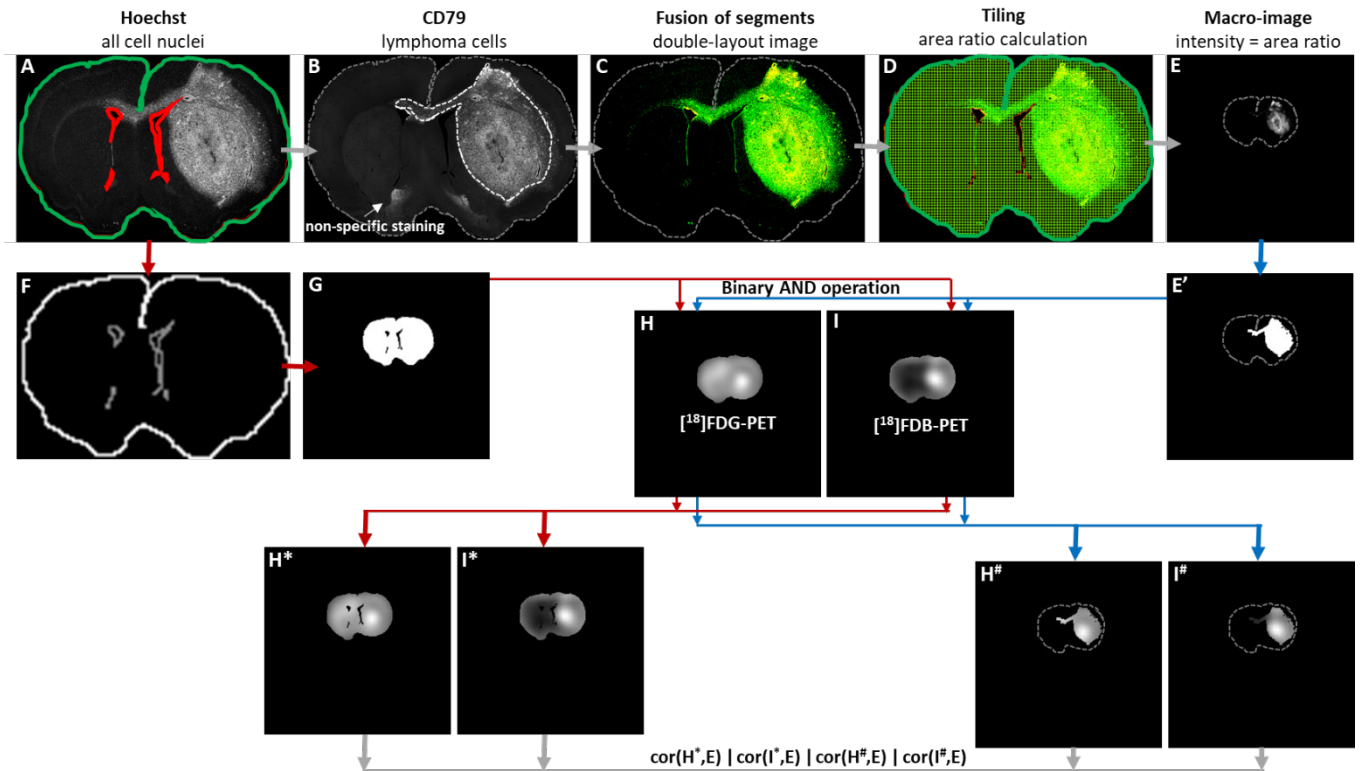
Supplementary Material
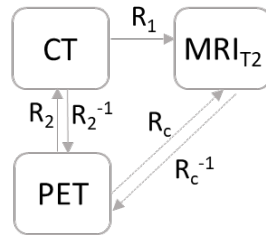
Figure S1: Image co-registration method.
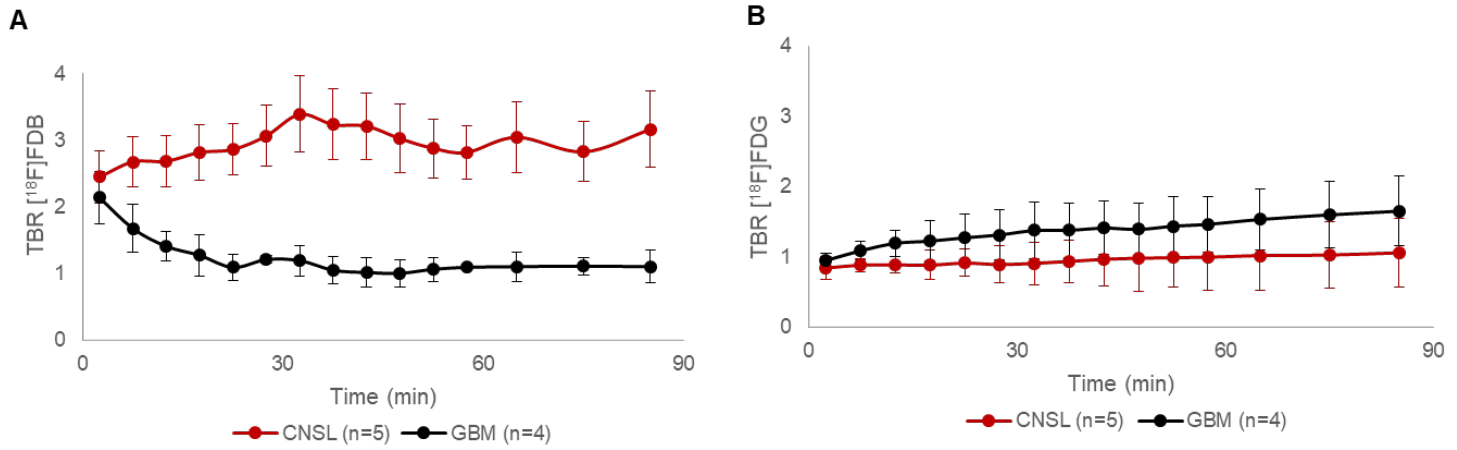
Figure S2: Time-activity curves. Dynamic changes in radiotracer accumulation with time, expressed as tumor-to-background ratio (TBR), in CNS lymphoma and GBM models for (**A**) [^{18}F]FDB- and (**B**) [^{18}F]FDG-PET. See Method 1 for data quantification in Supplementary Material.

Figure S3: Tile-based method of analysis explained on multimodal data of brain lymphoma model. A Hoechst-stained grey-level image. The manually drawn region of interest (ROI) is in green, the ventricle and the artifact exclusions are marked in red. To segment the stained cells, a background-constraint Entropy-based thresholding was applied. **B** CD79-stained grey-level image of the same brain section. The segmentation of the tumor cells is performed through the binary mask within the region (dotted white line) segmented on (A) in order to exclude the non-specific staining with CD79. **C** Fusion of the obtained segments (binary image): Hoescht in green and CD79 in yellow. **D** Subsampling of (C) by considering the initially defined ROIs. The size of a tile (square) is equal to the resolution of the reference image which is the T2w-MRI. **E** Resulted macro-image consisting of the computed pixels (ratio values calculated between the CD79-stained area in a tile and the surface of the tile) set in the reference space. **E'** Binary mask of the macro-image including the dense tumoral area. **F** Contours of the initially drawn ROIs, used for the creation of a binary mask. **G** Binary mask co-registered to the reference MRI image. **H** Corresponding [^{18}F]FDG- and **I** [^{18}F]FDB-PET scans pre-registered to MRI. **H***, **I*** Masked PET images to correlate with the macro-image (E) for total-section analysis (red track). **H$^{\#}$**, **I$^{\#}$** Masked PET images to correlate with the macro-image (E) for tumoral-zone analysis (blue track).

Notes: (i) To assess the correlation coefficient between two images, the intensity values were extracted and imported into an Excel file. The values were then filtered to remove the background (black = 0) which could lead to calculation bias in the correlation coefficient. (ii) Same protocol of analysis was applied on RECA stained images for vascular density evaluation and on CD68 stained images for calculating inflammatory cell density. (iii) The main part of the analysis (from A to E, as well as the extraction of intensity values from finalized images) were automatically processed with home-made scripts and home-made executable tools (windows shell scripts and compiled C programs (gcc freeware)). Histological images were displayed with Aperio ImageScope View 12.2 (Leica Biosystems, USA) for

visual control of features. All image co-registrations were performed with Pmod 3.7 (PMOD Technologies, Switzerland). Binary masks were manipulated with macro commands of ImageJ 1.51 (https://imagej.nih.gov/ij/).
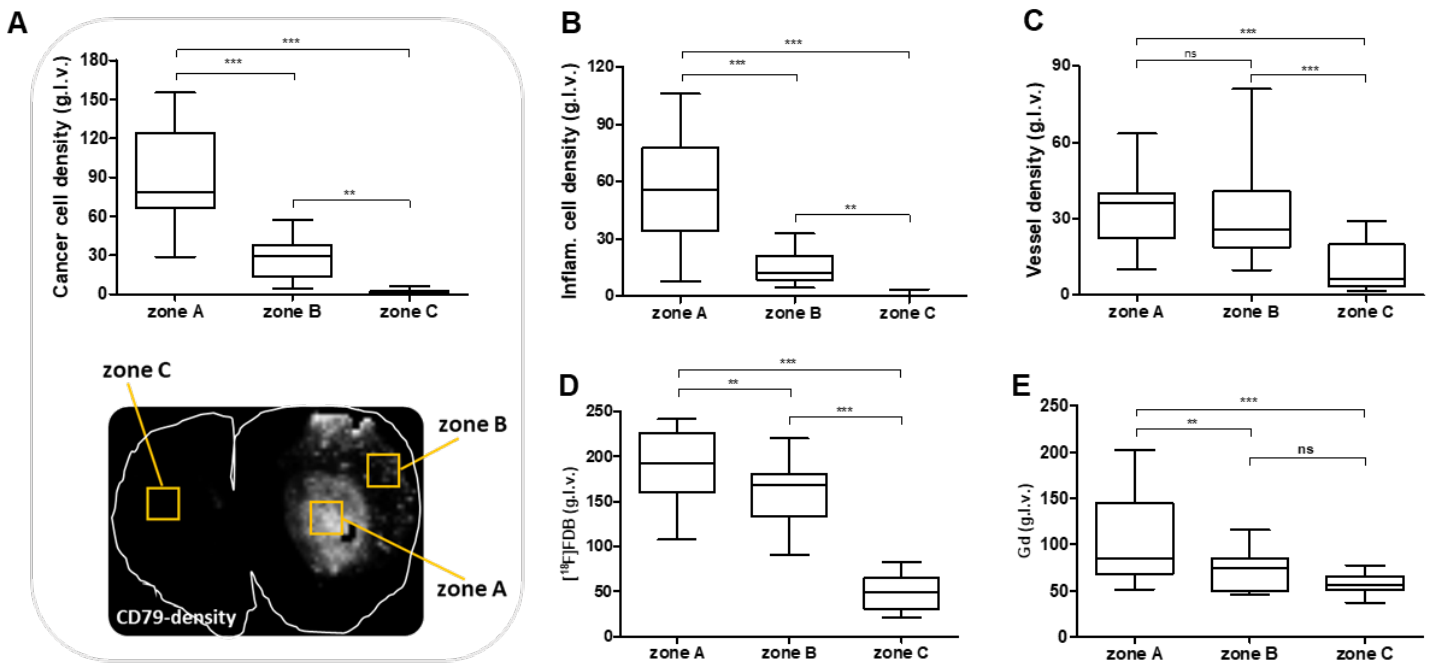
Figure S4: Quantitative data of tumor features based on multimodality. (**A**) Illustration of the region of interests (ROIs) including tumor core (zone A), tumor periphery (zone B) and normal tissue (zone C) and the corresponding chart of the cancerous cell-density (CD79 staining). (**B**) Inflammatory cell-density (CD68 staining) and (**C**) morphological analysis of vessels regarding the vascular surface density (RECA staining) in the defined regions. (**D**) [^{18}F]FDB (average 40-60 min) and (**E**) Gd accumulation in the corresponding zones. All scans were converted to greyscale images (g.l.v.: grey-level value). *** $p < 0.001$, ** $p < 0.01$, ns $p > 0.05$ one-factor ANOVA followed by Bonferonni. See Method 4 for data quantification in Supplementary Material.